

1 Enabling portable multiple-line refreshable Braille displays with  
2 electroactive elastomers

3  
4 Gabriele Frediani<sup>a</sup>, James Busfield<sup>b</sup>, Federico Carpi<sup>a,\*</sup>

5  
6 <sup>a</sup> *University of Florence, Department of Industrial Engineering, Via di S. Marta, 3 - 50139 Florence, Italy.*

7 <sup>b</sup> *Queen Mary University of London, School of Engineering & Materials Science, Mile End Road, E14NS, London, UK.*

8  
9  
10  
11  
12  
13 Medical Engineering and Physics 60 (2018) 86–93

14 <https://doi.org/10.1016/j.medengphy.2018.07.012>

15  
16  
17  
18 **ACCEPTED VERSION**

19  
20  
21  
22  

---

\* Corresponding author. Tel.: +39 055 2758660;  
E-mail address: federico.carpi@unifi.it.

23 **Abstract**

24

25 Full-page (multiple-lines), electrically refreshable, portable and affordable Braille displays do not currently exist.  
26 There is a need for such an assistive technology, which could be used as the Braille-coded tactile analogue for blind  
27 people of the digital tablets used by sighted people. Turning those highly desirable systems into reality requires a  
28 radically new technology for Braille dot actuation. Here, we describe standard-sized refreshable Braille dots based on  
29 an innovative actuation technology that uses electro-responsive smart materials known as dielectric elastomers. Owing  
30 to a significantly reduced lateral size with respect to conventional Braille dot drives, the proposed solution is suitable  
31 to array multiple dots in multiple lines, so as to form full-page Braille displays. Furthermore, a significant reduction  
32 also of the vertical size makes the design suitable for the development of thin and lightweight displays, thus enabling  
33 portability. We present the first prototype samples of these new refreshable Braille dots, showing that the achievable  
34 active displacements are adequately close to the standard Braille requirements, although the force has to be further  
35 improved. The paper discusses the remaining challenges and describes promising strategies to address them.

36

37 *Keywords:* actuator; braille; blind; dielectric elastomer; display; electroactive; multiple line; polymer; portable; refreshable; tactile.

38

39

---

## 40 **1. Introduction**

41

42 The world's roughly 314 million blind and visually impaired people are largely excluded from today's  
43 digital revolution in information and communication technologies. Indeed, displays of computers, portable  
44 devices, touch screens and so forth are conceived to bring text and images via the sense of sight.

45 Visually impaired people can access digital information only via text-to-speech readers. However,  
46 conveying information using sound is not always effective. Indeed, the interpretation of text based only on  
47 listening might be limited, for example, by the impossibility of a continuous backtrack. Furthermore, the  
48 presence of other people nearby might require the use of headphones to protect privacy or not to disturb,  
49 whilst a noisy environment might provide an additional challenge.

50 Overcoming these problems requires refreshable Braille displays. They are conceived as electronically  
51 controllable tactile interfaces allowing blind users to read text presented in the Braille code via dots that are  
52 dynamically raised and lowered. In particular, full-page displays would allow blind people to access via the  
53 sense of touch large amounts of structured and dynamic information, like sighted people commonly do via  
54 the sense of sight, for example when using computer monitor displays, tablets and smartphones. In other  
55 words, full-page displays are needed as the Braille-coded tactile analogue for the blind people of the  
56 displays used by the sighted people to visualise text and images.

57 Commercially available refreshable Braille displays are based on piezoelectric reeds that actuate the  
58 Braille dots. The reeds are mounted as a stair stepped stack of cantilevers, each with a Braille pin resting on  
59 its free end [1]. This solution limits the whole display to a maximum of two lines of Braille characters [2],  
60 which makes backtracking impossible while reading a full page of text. To overcome this limitation,  
61 attempts to develop full-page Braille readers based on different types of piezoelectric actuators are in  
62 progress, although the only available system developed so far is non-portable and has an estimated cost of  
63 about € 60,000 [3].

64 So, affordable, portable and multiple-line (full-page) Braille displays are needed, as they merely  
65 represent technological fiction today. They are required to facilitate access to digital information, as well as  
66 to help to improve the Braille literacy rate across the blind population, also with the aim of reducing its  
67 high unemployment rate [4].

68 A paradigm shift from technological fiction to reality requires the ground-breaking creation of a radically  
69 new technology for Braille dot actuation. To this end, several alternatives to piezoelectric actuators have  
70 been studied. For instance, pneumatically actuated Braille dots with microvalves have been proposed [5],  
71 although the need for air pumping and individual dot control limits the portability of the resulting systems.  
72 Shape memory alloys have also been investigated as a method of providing actuation, although they show  
73 limitations in terms of size, speed and power consumption [6]. Linear actuators vertically pushing Braille  
74 dots have been prototyped using either rolled sheets of electrostrictive polymers [7] or tubes of dielectric  
75 elastomers [8], although the length of the actuators enlarges the size of the device.

76 Dielectric elastomer (DE) actuators [9-11] represent the electromechanical transduction technology used  
77 in this work too. They belong to the bigger family of electromechanically active polymers [12], which  
78 includes a diversity of smart materials studied for various biomedical applications [13]. The most basic  
79 configuration of a DE actuator consists of a thin elastomeric layer coated with two compliant electrodes, so  
80 as to obtain a deformable capacitor. A voltage  $V$  applied between the electrodes results in the following  
81 effective electrostatic pressure  $p$  on the elastomer surface:

$$82 \quad p = \epsilon_r \epsilon_0 \left(\frac{V}{d}\right)^2 \quad (1)$$

83 where  $\epsilon_0$  is the dielectric permittivity of vacuum,  $\epsilon_r$  is the elastomer's relative dielectric constant and  $d$  is  
84 the dielectric layer's thickness. This pressure causes a squeezing in thickness and a concurrent surface  
85 expansion [11].

86 The DE actuation technology in general offers attractive properties in terms of large strains, fast, stable  
87 and silent operation, compact size, low weight, shock tolerance, low power consumption and no  
88 overheating [9-11, 14]. DE actuators show significant potential to develop compact, fast, lightweight and  
89 silent electromechanical transducers for tactile interfaces [14]. Studied configurations include cylinders [7,  
90 8, 15], diaphragms [16], buckling membranes [17, 18], planar multi-layer stacks [19] and bistable  
91 diaphragms [20]. Nevertheless, so far, none of these proposed configurations seems to be readily applicable  
92 to obtain commercially viable Braille displays. This is due to a number of challenges (specific to each  
93 approach), related to one or more of the following drawbacks: low forces, low displacements, low response  
94 speed, high cell thickness and overall encumbrance, high energy consumption, overheating, manufacturing  
95 complexity, short lifetime, low reliability (see details in the previously mentioned references).

96 Aimed at overcoming the limitations of these state-of-the-art approaches, this paper presents real-size  
97 refreshable Braille dots based on DE actuation. The design, working principle, fabrication and a  
98 preliminary electromechanical characterization are described in the next sections, following a reminder of  
99 the main technical requirements.

100

## 101 **2. Technical specifications**

102

103 The requirements in terms of dimensions and force for a standard Braille dot [1] are presented in Table 1.

104 Table 1

105 Specifications of Braille dot parameters for refreshable Braille displays [1].

<b>Dot</b>	<b>Typical</b>
<b>parameter</b>	<b>value</b>
Base diameter	1.5 mm
Height (assuming no force from user's finger)	0.7 mm
Blocking force (dot raised within 0.1 mm of maximum height)	50 mN
Blocking force (dot raised 0.25 mm above reading surface)	150 mN

106

107 According to these requirements, the raised Braille dot consists of a quasi-hemispherical cap.

108 Moreover, besides these geometrical and performance requirements, the dots' actuation technology  
109 should comply with electrical safety issues and allow for ease of miniaturization at low production costs, so  
110 as to enable compact and cost-effective systems.

111 Aimed at addressing such needs, this paper presents the concept and a prototype implementation of a  
112 radically new kind of Braille dots with intrinsic dynamic actuation.

113

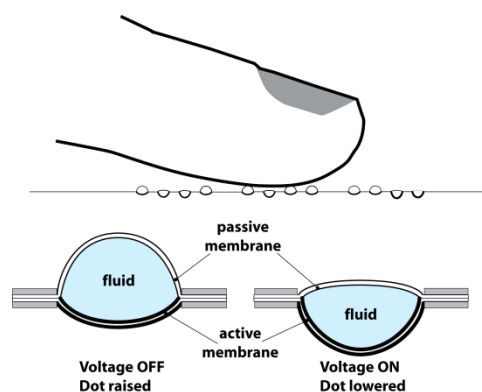
## 114 **3. Proposed concept and principle of operation**

115

116 The concept is based on the particular type of DE technology known as 'hydrostatically coupled' DE  
117 (HC-DE) actuation [21]. HC-DE actuators in general are based on an incompressible fluid that

118 mechanically couples a DE-based active part to a passive part interfaced to the load, so as to enable  
119 hydrostatic transmission. This general concept was used in this work to conceive a dynamic Braille dot as a  
120 bubble-like HC-DE actuator. The device is such that the actuator itself coincides with the dynamic Braille  
121 dot. The structure is shown in Fig. 1.

122



123

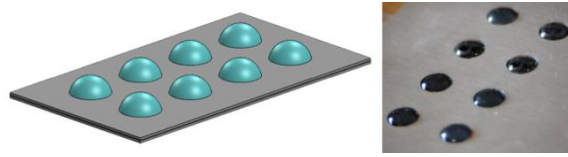
124 Fig. 1. Schematic drawing of the proposed concept. In order to obtain an array of electrically controllable compact Braille dots (top panel), each dot  
125 consists of a bubble-like HC-DE actuator (bottom panel). A lateral section of the actuator/dot is shown in the rest state (bottom, left) and in an  
126 electrically induced state due to an applied voltage (bottom, right).

127

128 It includes the following parts: an electromechanically active membrane, made of a DE film coated with  
129 compliant electrodes; an electromechanically passive membrane, working as the end effector in contact  
130 with the finger (either directly, or via any interposed medium); an incompressible fluid contained in a  
131 chamber constrained by the two membranes. Both membranes are radially constrained by bonding them to  
132 a frame, in the region external to the chamber. The internal fluid is pressurised during manufacturing, so as  
133 to provide each membrane with the shape of a roughly spherical cap. The pressurised top membrane works  
134 as the Braille cell dot (passive interface with the user's fingertip). The pressurised bottom membrane  
135 behaves as a buckling DE actuator. The latter buckles outwards as a voltage difference is applied between  
136 its electrodes, while the passive membrane relaxes (as the pressure is reduced) and passively moves  
137 inwards, according to the fluid-enabled hydrostatic transmission (Fig. 1). Therefore, the dot is lowered or  
138 raised as a voltage is applied or removed, respectively. This principle allows for an electrically safe  
139 transmission of actuation from the active membrane to the finger, without any direct contact between them.

140 This basic structure can be replicated to implement a standard 8-dots Braille cell, as shown in Fig. 2.

141



142

143 Fig. 2. Array of eight Braille dots based on the proposed configuration, to obtain a dynamic Braille cell: concept (left) and assembled prototype  
144 (right).

145

146 Prototype dots were manufactured and tested as described in the next sections.

147

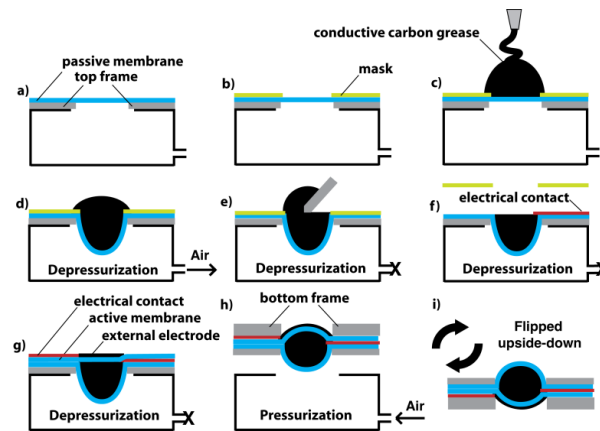
## 148 4. Materials and methods

149

### 150 4.1 Manufacturing

151 The fabrication process consisted of several steps, which are presented in Fig. 3 and are described below.

152



153

154 Fig. 3. Braille dot fabrication steps. A dielectric elastomer membrane previously bonded to a PMMA frame is placed over an empty chamber  
155 containing a circular hole (a); the membrane is masked, such that the central circular portion, corresponding to the chamber's hole, is left exposed  
156 (b); the membrane is coated with conductive carbon grease (c); a depressurization is applied inside the chamber in order to deform the membrane  
157 (d); the excess grease is removed (e); the mask is peeled off and the internal electrical contact is applied (f); a second dielectric elastomer  
158 membrane is arranged above, a thin layer of carbon grease is deposited on top of it and an electrical contact is created (g); a second circular frame  
159 is applied above and the chamber is brought back to atmospheric pressure to release the overstress applied to the passive membrane and detach the  
160 obtained structure from the chamber (h); the structure is flipped upside down to be used as a Braille dot (i).

161

162 The actuator was assembled using membranes made of commercially available acrylic elastomer films  
163 (VHB tape series, by 3M). In particular, four combinations of different grades were tested, as detailed in

164 the next section.

165 Each membrane was bi-axially pre-stretched by four times, which means that it was subjected to a biaxial  
166 pre-strain of 300%. The application of this pre-strain was justified as a consequence of the well-known  
167 beneficial effect that consists in an increase in the electromechanical transduction performance, as first  
168 documented by Pelrine et al. [11] and later on explained in different ways by Brochu and Pei [9] and Koh  
169 et al. [22].

170 The pre-stretched membrane that had to work as the passive membrane was coupled to a thin metallic  
171 support frame, exploiting the fact that their bonding was ensured by the adhesive properties of the  
172 membrane's constitutive material. This membrane and its support were then placed over a vacuum chamber  
173 (Fig. 3a). An annular mask was applied to the membrane, in order to leave its central circular portion,  
174 corresponding to the chamber's hole, exposed (Fig. 3b). To this end the paper liner that came with the VHB  
175 tape was used, so as to facilitate the mask removal afterwards. Then, the membrane was coated with a  
176 carbon conductive grease (846, M.G. Chemicals, Canada) (Fig. 3c), which was used both as the hydrostatic  
177 coupling fluid and the internal electrode for the active membrane; the volume of deposited grease was  
178 intentionally in excess, in order to simplify the subsequent steps of the process and ensure adequate filling  
179 of the bubble cavity to be created. Afterwards, the chamber was depressurised in order to deform the  
180 membrane, so as to obtain a cavity filled in by the grease (Fig. 3d). This procedure avoided that any air  
181 bubble remained trapped at the membrane/grease interface, as it would likely be the case if the grease were  
182 applied after the creation of the cavity. Subsequently, the excess grease was removed (Fig. 3e), the mask  
183 was peeled off and a thin aluminium strip was applied to serve as the internal electrical contact (Fig. 3f).  
184 The structure was covered with the prestretched membrane that had to work as the active membrane (again  
185 exploiting its inherent adhesive properties), which was then coated with the same type of carbon conductive  
186 grease to create the external electrode; then, an aluminium strip was applied to create the external electrical  
187 contact (Fig. 3g). A second PMMA frame was finally coupled to the active membrane and the so-obtained  
188 actuator was removed from the vacuum chamber by pressurising it (Fig. 3h,i).

189 The resulting shape of the stabilised final structure was asymmetric (with the heights of the active and  
190 passive caps being different, as shown in Fig. 3i), as a consequence of the following two concomitant  
191 effects. First, the stiffness of the two membranes was different, due to a difference in the thickness of the



192 adopted films (according to the values reported in the next section). Second, the Mullins effect [23] caused  
193 a stretch-induced softening of the passive membrane, due to the overstretch imposed during the  
194 depressurisation phase.

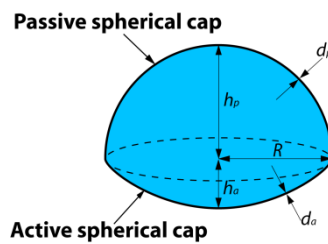
195 As the asymmetry of the device was expected to influence its performance, different prototypes with  
196 passive and active caps of different heights were assembled and compared. To this end, membranes made  
197 of three types of films having different initial thickness were used, evaluating four combinations, as  
198 described in the next section.

199

#### 200 4.2 Comparisons among four sets of prototypes with different active cap height

201 From a geometrical standpoint, the conceived dynamic Braille dot can be regarded as the union of two  
202 ideally spherical caps, having the same base radius  $R$  but different heights  $h_a$  and  $h_p$  at electrical rest (no  
203 applied voltage), as represented in Fig. 4.

204



205

206 Fig. 4. Schematic geometrical representation of the proposed Braille dot.

207

208 The active and passive membranes have at electrical rest a thickness  $d_a$  and  $d_p$ , respectively.

209 In order to meet the geometrical Braille requirements, the dots were manufactured with a base radius  
210  $R=750 \mu\text{m}$  and a passive cap height  $h_p$  of approximately  $750 \mu\text{m}$ .

211 As the active cap height  $h_a$  was a free parameter for the actuator design, in this study its effect on the  
212 resulting performance was investigated by manufacturing four sets of different dots, made of different  
213 combinations of elastomers frequently employed for DE actuators in general. In particular, the four sets  
214 were obtained by using, as active and passive membranes, the following commercially available acrylic  
215 films by 3M: VHB 4910, VHB 4905 and VHB 9473PC. The tested combinations are presented in Table 2.

216

217

Table 2.

Actuator set	Active membrane	Passive membrane
1	VHB 4910	VHB 4905
2	VHB 4910	VHB 9473PC
3	VHB 4905	VHB 4905
4	VHB 4905	VHB 9473PC

219

220 During manufacturing, while the active cap height  $h_a$  was not controlled, the passive membrane was  
 221 processed in such a way that the final passive cap height  $h_p$  was as close as possible to the targeted 750  $\mu\text{m}$   
 222 for each set of prototypes. To this end, the applied depressurization (Fig. 3d) was empirically adjusted to a  
 223 different level for each set. Adjustments were required, due to the different values of stiffness shown by the  
 224 two membranes used in each set, as a consequence of their different thickness. Indeed, the thickness of the  
 225 initial elastomer films in the non-stretched state was 1000, 500 and 250  $\mu\text{m}$ , respectively for VHB 4910,  
 226 4905 and 9473PC, which then, upon the application of a 300% biaxial pre-strain, respectively reduced to  
 227 about 62.5, 31.3 and 15.6  $\mu\text{m}$  (calculated values). The thickness then further reduced as a result of the  
 228 actuator assembly, owing to the hemispherical shaping of the membranes. The final values of the  
 229 membrane thicknesses were computed as described in the next section.

230

### 231 4.3 Geometrical estimate of the thickness of the two membranes

232 A simple geometrical analysis of the structure allows for estimating  $d_a$  and  $d_p$  from measured values of  $h_a$   
 233 and  $h_p$ . Prior to providing the two membranes with a three-dimensional shape (while manufacturing the  
 234 device), they initially consisted of flat circular elastomeric layers having a radius  $R$  and an initial thickness  
 235 (immediately after the 300% biaxial prestretch) of  $d_{a,0}$  and  $d_{p,0}$ , respectively. So, their initial surface  $S_0$  and  
 236 volumes  $Vol_{a,0}$  and  $Vol_{p,0}$  were:

$$237 \quad S_0 = \pi R^2 \quad (2)$$

$$238 \quad Vol_{a,0} = S_0 d_{a,0} \quad (3)$$

$$239 \quad Vol_{p,0} = S_0 d_{p,0} \quad (4)$$

240 During the fabrication of the device, the active and passive membranes were deformed, such that their  
241 final shapes were ideally spherical caps, with surfaces  $S_a$  and  $S_p$ , respectively, given by the following  
242 expressions:

$$243 \quad S_a = \pi(R^2 + h_a^2) \quad (5)$$

$$244 \quad S_p = \pi(R^2 + h_p^2) \quad (6)$$

245 Furthermore, by considering that the thickness of the two membranes was negligible with respect to the  
246 cap height and base radius, the final volumes of the membranes  $Vol_a$  and  $Vol_p$ , respectively, could be  
247 approximated as follows:

$$248 \quad Vol_a \cong S_a d_a \quad (7)$$

$$249 \quad Vol_p \cong S_p d_p \quad (8)$$

250 Moreover, by assuming that each elastomeric membrane maintained a constant volume under  
251 deformation, the following can be seen:

$$252 \quad S_0 d_{a,0} = S_a d_a \quad (9)$$

$$253 \quad S_0 d_{p,0} = S_p d_p \quad (10)$$

254 Therefore, the final thickness of the membranes could be obtained as follows:

$$255 \quad d_a \cong d_{a,0} \frac{R^2}{(R^2 + h_a^2)} \quad (11)$$

$$256 \quad d_p \cong d_{p,0} \frac{R^2}{(R^2 + h_p^2)} \quad (12)$$

257

#### 258 *4.4 Measurement of the blocking force and stress relaxation*

259 For each combination of active and passive membranes, three samples were manufactured and  
260 characterised in terms of blocking force and stress relaxation.

261 The blocking force was defined as the force generated by the Braille dot for a given applied  
262 displacement. It was measured with a double-column dynamometer (Z005, Zwick Roell, Germany), as  
263 follows. A cylindrical indenter, having a diameter of 2 mm, was connected to the machine's load cell

264 mounted on a mobile crossbar. The indenter was brought in contact with the Braille dot apex and the  
265 crossbar was displaced and maintained at a given position, so as to maintain the apex displaced, for 30  
266 seconds, while the variation of force was recorded over time. The apex displacement corresponded to an  
267 indentation of the Braille dot. Measurements were taken for two values of indentation, 100 and 500  $\mu\text{m}$ , as  
268 recommended in [1]. This procedure allowed for quantifying the force (and its relaxation over time) with  
269 which the Braille dot tends to resist the tactile action exerted by the user.

270

#### 271 *4.5 Measurement of the free stroke*

272 Three samples for each combination of active and passive membranes were also characterised in terms of  
273 their free stroke, i.e. their voltage-induced displacement.

274 To this end, the displacement of the Braille dot apex, corresponding to an electrically generated reduction  
275 of the passive cap height, was measured using a laser-based displacement transducer (optoNCDT1800,  
276 Micro-Epsilon, Germany), according to general recommendations for free stroke measurements of DE  
277 actuators [24]. The free stroke was determined for step-wise voltages, whose amplitudes were varied with  
278 steps of 250 V, up to the actuator's electrical breakdown (which changed according to the active membrane  
279 thickness). The corresponding maximum applied voltages (average values) for the actuator sets 1, 2, 3 and  
280 4 (Table 2) were, respectively, 4.5, 4.5, 2.25 and 2.5 kV.

281

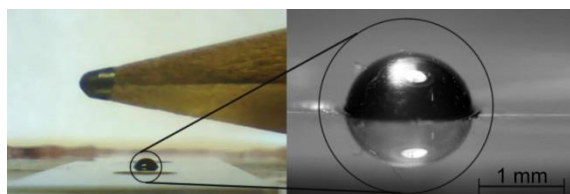
## 282 **5. Results**

283

### 284 *5.1 Prototype samples of Braille dot*

285 A prototype sample of the Braille dot is shown in Fig. 5.

286



287

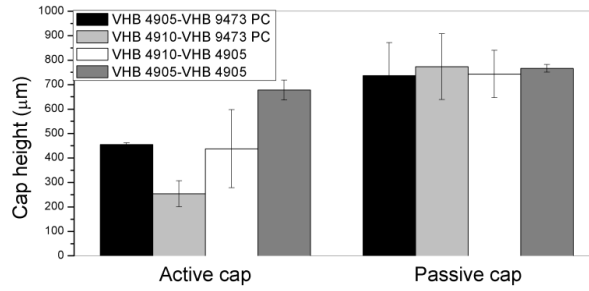
288

Fig. 5. Pictures of a prototype Braille dot at electrical rest.

289

290 Fig. 6 presents the measurements of the active and passive cap heights  $h_a$  and  $h_p$  at electrical rest (i.e.  
 291 without any applied voltage) for the four sets of manufactured Braille dots.

292



293

294 Fig. 6. Average active and passive cap heights  $h_a$  and  $h_p$  at electrical rest, for the four sets of prototype Braille dots. Error bars represent the  
 295 standard deviation related to the three samples tested for each set.

296

297 As shown by these data, the average passive cap height was about 750 µm for each set of prototypes, as  
 298 intended. However, the active caps had a variable height, according to the differences in the stiffness of the  
 299 membranes, due to the combination of different materials.

300 The average values of the cap heights were used to compute the average values of the thickness of the  
 301 active and passive membranes, for each combination of materials, according to Eqs. (11) and (12). The  
 302 computed values for the four sets of prototypes are presented in Table 3.

303

304

305

Table 3.

Average values at electrical rest of the thickness of the active and passive membranes.

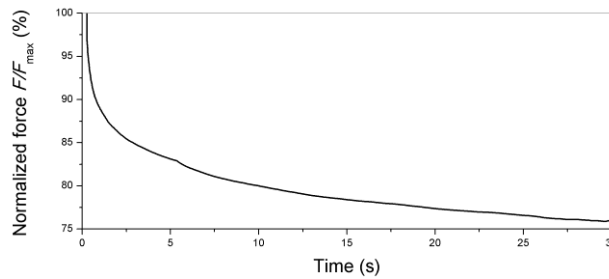
		Active membrane	
		VHB 4910	VHB 4905
Passive membrane	VHB 4905	$d_a=48.07 \mu\text{m}$ $d_p=18.37 \mu\text{m}$	$d_a=18.2 \mu\text{m}$ $d_p=16.31 \mu\text{m}$
	VHB 9473 PC	$d_a=56.6 \mu\text{m}$ $d_p=8.14 \mu\text{m}$	$d_a=23.6 \mu\text{m}$ $d_p=8.56 \mu\text{m}$

306

307 5.2 Braille dot blocking force

308 Owing to the viscous nature of the elastomeric materials used to make the Braille dots, the four sets of  
309 prototype Braille dots were found to exhibit a significant stress relaxation. Fig. 7 presents results of a  
310 typical relaxation test.

311



312

313 Fig. 7. Typical relaxation of the force generated by the Braille dot, for a given applied displacement.

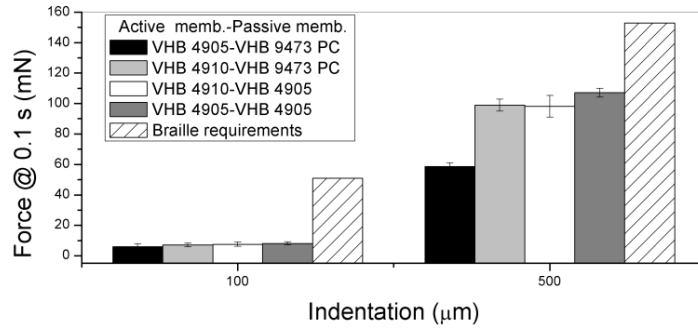
314

315 In particular, the prototype dots exhibited a typical decrease in force of about 25% after 30 seconds.

316 Notwithstanding such a considerable drop of force over time, it is worth noting that the value at 30  
317 seconds is not representative of the force that a user would actually experience while reading a Braille text.  
318 Indeed, Braille reading occurs via continuous movements of the finger over the dots, such that they are  
319 never solicited statically. The relevant variable is the time needed to slide the finger over a single dot, in  
320 order to estimate its height. This time can be evaluated as the mean time needed to read a letter (which for a  
321 Braille system is a group of eight dots), and it can be estimated as follows. Considering a reading rate of  
322 100 words per minute [25] and an average of 5.1 letters per word in the English language [26], the resulting  
323 reading speed is 510 letters per minute, i.e. 8.5 letters per second. This implies that the user touches a new  
324 group of eight Braille dots approximately every 0.1 s. Therefore, it is important that the dot response in  
325 terms of force is guaranteed within about 0.1 s from the beginning of the contact with the finger.

326 So, the relevant values of force to be considered from the electromechanical characterisation are those  
327 measured at 0.1 s after the indentation onset. They are presented in Fig. 8, where they are also compared  
328 with the Braille requirements [1].

329



330

331 Fig. 8. Average blocking force at electrical rest, shown by each prototype Braille dot 0.1 s after its indentation. Values are reported for two levels of  
 332 indentation. Error bars represent the standard deviation related to the three samples tested for each set of prototypes.

333

334 *5.3 Voltage-induced Braille dot displacement*

335 An electrically induced displacement of a prototype Braille dot is shown in Fig. 9.

336



337

338 Fig. 9. Picture of a prototype Braille dot at rest (left) and when a voltage is applied (right). A video of the dot in action is available at

339

<https://www.youtube.com/watch?v=8mSCbKITcO0>.

340

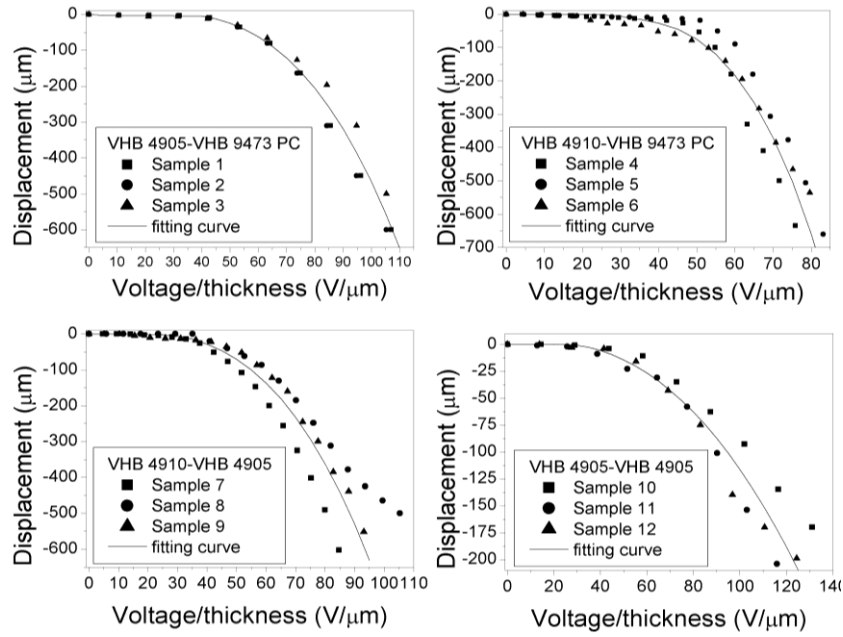
341 The typical response time to reach 90% of the final dot height was about 2 s.

342 Fig. 10 presents, for each set of prototypes, the steady-state electrically-induced displacement of the

343 Braille dot apex, as a function of the voltage normalised by the active membrane thickness at electrical rest

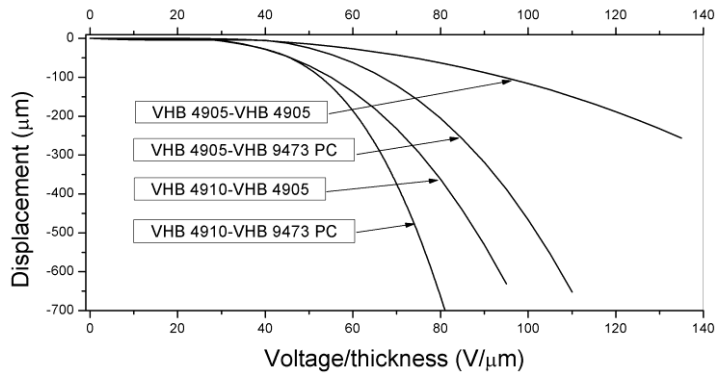
344  $d_a$ .

345



346  
 347 Fig. 10. Voltage-induced displacement of the Braille dot apex for the four sets of prototype dots. A data fitting line for each set is used as a guide  
 348 for the eye.

349  
 350 For the sake of a direct comparison of the performance shown by the four sets of prototype dots, Fig. 11  
 351 presents a co-plot of the fitting lines extracted from Fig. 10.

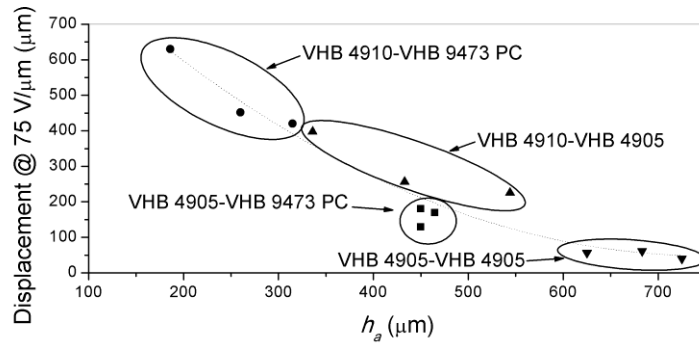


352  
 353 Fig. 11. Comparison of the actuation performance of the four sets of prototype Braille dots.

354  
 355  
 356 The effect of the active cap height at electrical rest  $h_a$  on the achievable displacement is presented in Fig.  
 357 12, which plots the displacement at  $75 \text{ V}/\mu\text{m}$  (arbitrarily chosen as a reference value from Fig. 11), as a  
 358 function of the cap height for each sample of each set of Braille dots.

359





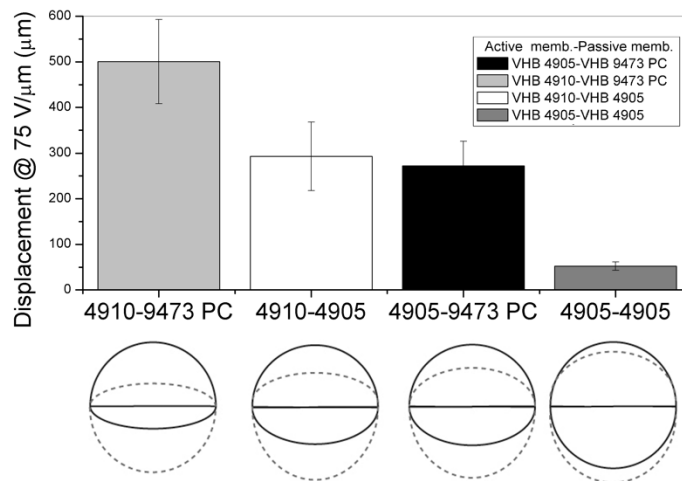
360

361 Fig. 12. Braille dot apex displacement obtained at 75 V/μm as a function of the active cap height at electrical rest, for each prototype Braille dot.

362

363 The average value of the displacements at 75 V/μm is shown, for each set of prototypes, in Fig. 13, which  
 364 also displays the related asymmetry of the dots in the active and passive states.

365



366

367 Fig. 13. Average displacement at 75 V/μm for the four sets of prototype Braille dot. Error bars represent the standard deviation related to the three  
 368 samples tested for each set. The schematic drawing associated to each set represents, qualitatively, a cross-section of the asymmetric dot in the  
 369 passive state (solid line) and active state (dotted line).

370

371

372

## 373 **6. Discussion**

374

### 375 *6.1 Compact size enabling multiple-line portable displays*

376 As compared to commercial systems, the design proposed here has the unique advantage of fusing in the  
377 same structure the Braille dot and its driving mechanism.

378 The consequent significant reduction of the lateral size of the actuation part makes the proposed solution  
379 suitable to the creation of an array of multiple dots in multiple lines, as required by the development of full-  
380 page Braille displays. Furthermore, the significant reduction also of the vertical size makes the design  
381 potentially suitable to obtain thin and lightweight displays, thus enabling portability, possibly also creating  
382 hand-held devices.

383

### 384 *6.2 Achievable blocking force*

385 Fig. 8 shows that, in order to comply with Braille requirements in terms of blocking force, further  
386 improvements are necessary. Indeed, although for some Braille readers with light touch the force generated  
387 by these prototypes might be sufficient, for others it may result in a so-called tactile noise [1]. Increasing  
388 the dot's passive (i.e. elastic or, better, hyperelastic) force requires a stiffening of the membranes.

389 This could be obtained in different ways. While using stiffer elastomers and/or thicker passive  
390 membranes would be a simple approach, it is not advisable as it would reduce the achievable active  
391 displacements. Moreover, if applied to the active membrane, it would also increase the required driving  
392 voltage. To avoid these drawbacks, a more promising, although even more challenging, strategy is to create  
393 a multi-layered active membrane, by stacking multiple dielectric films intertwined to multiple compliant  
394 electrodes. This would increase the active membrane total thickness, while preserving a low separation  
395 between the electrode pairs so as not to increase the required driving voltage.

396

### 397 *6.3 Achievable displacement*

398 As expected, the asymmetry of the Braille dot influenced its performance in terms of achievable  
399 displacement (Fig. 13). In particular, the average displacement at  $75 \text{ V}/\mu\text{m}$  was about  $500 \mu\text{m}$  for the set

400 VHB 4910-VHB 9473PC, which had the lowest height of the active cap at rest. The dots with increasing  
401 values of that height showed decreasing displacement.

402 This evidence could be interpreted by assuming that the flatter active caps corresponded to less stretched  
403 active membranes, which were therefore less stiff (it is worth noting that during manufacturing each  
404 membrane was bi-axially pre-stretched above the flex point of its stress-strain curve). The lower stiffness  
405 determined a higher active deformation in response to any given electrical stimulus.

406 It is worth noting that the softest set of dots did not show the highest deformation. Indeed, the stiffness  
407 inferable from data reported in Fig. 8 is not representative of the stiffness of the active membrane only.

408

#### 409 *6.4 Selection of the best trade-off configuration*

410 The set of prototypes VHB 4910-VHB 9473PC offered the best trade off in terms of performance.  
411 Indeed, as shown in Figs. 8 and 12, it allowed for a maximisation of the displacement while providing a  
412 force just 10% smaller than the maximum value recorded.

413

#### 414 *6.5 High voltage driving*

415 One of the major drawbacks of the proposed technology is represented by the need for high driving  
416 voltages. This introduces a limitation in terms of size, safety and cost of the required electronics, as  
417 discussed below.

418 The generation of voltages as high as those used in this work is *per se* not particularly problematic from a  
419 technical standpoint or particularly dangerous in terms of electrical safety, considering that there is no need  
420 for high driving powers (the loads are capacitive) and that all the high-voltage parts are insulated. Indeed,  
421 the generation of voltages of the order of 1 kV has been demonstrated for micro-battery powered systems  
422 using compact voltage multipliers, as discussed in [27], enabling the development of single-channel  
423 systems that are both portable and relatively safe.

424 However, the electrical driving of arrays of multiple actuators is more challenging, as it implies the  
425 control of several high-voltage channels. The most straightforward approach that could be considered  
426 requires the use of one high voltage converter for each actuator, but this would excessively increase the  
427 size, cost and power consumption of the system. Overcoming this problem requires the adoption of driving

428 strategies specifically designed for this application. An example could consist in multiplexing a single  
429 high-voltage source (for example by using high voltage MOSFETs) while using the control strategy called  
430 Dynamic Scanning Actuation proposed by Koo et al. [28]. With that strategy, one line of the array delivers  
431 the high voltage, while a second line is grounded. Actuation is triggered only when both the lines are  
432 active, so that, by sequentially scanning each line, it is possible to continuously refresh each actuator's  
433 state, setting it to the desired value (on or off).

434 Notwithstanding such approaches for the driving electronics, the major drawbacks are still represented  
435 by its size and cost, since, as compared to low-voltage units, high-voltage components are more difficult to  
436 miniaturise and have relatively lower market share. So, the reduction of the driving voltage is imperative in  
437 order to unleash the real potential of the DE actuation technology for Braille displays.

438 To this end, future developments should be aimed at lowering the voltages down to about 200 V, which  
439 is the standard for the low-cost and low-size drives of piezoelectric transducers (available in a huge  
440 diversity of products today). To address this need, according to Eq. (1) there are two strategies: i) synthesis  
441 of new elastomers with higher dielectric constant [29, 30]; ii) processing the elastomers as thinner films.  
442 Reaching these targets requires the use of silicone elastomers, as in general they combine ease of material  
443 processing with very low viscosity that enables a higher actuation speed [31]. Custom manufacturing  
444 processes are necessary to reduce the thickness ideally down to a few microns. Although this is challenging  
445 for highly stretchable materials, preliminary evidences indicate feasibility [32]. On the other hand, in order  
446 to avoid a reduction of the elastic force due to the reduction of the active membrane thickness, it will be  
447 necessary to create a multi-layer structure, as discussed previously.

448

#### 449 *6.6 Other uses of the proposed new technology*

450 The actuation technology presented here might be considered also for other types of tactile displays, not  
451 necessarily intended for the blind people. For instance, arrays of tactile elements might be integrated within  
452 user interfaces and control panels, to enable tactile feedback aimed at enhancing human-machine  
453 interactions.

454

455 **7. Conclusions**

456

457 In this work we presented a concept to enable the development of dynamic Braille dots for multiple-lines  
458 refreshable Braille displays that can be portable and affordable. Prototype samples of these new refreshable  
459 Braille dots were assembled using off-the-shelf materials and adopting tools and procedures not yet  
460 optimised. Whereas the prototypes allowed for a proof-of-concept demonstration of the functionality of the  
461 proposed concept, they also showed the required future improvements. These include the need for  
462 processing more suitable elastomers as thinner films and using them to assemble multi-layer structures,  
463 which should be extensively characterised also in terms of cycle lifetime. Overall, these suggested  
464 developments define a road map towards the first Braille tablets.

465

466 **Competing interests**

467 None declared

468

469 **Funding**

470 None

471

472 **Ethical approval**

473 Not required

474

475 **References**

476

- 477 [1] N. H. Runyan, and F. Carpi, "Seeking the 'holy Braille' display: might electromechanically active polymers be  
478 the solution?," *Expert Review of Medical Devices*, vol. 8, no. 5, pp. 529-532, 2011.
- 479 [2] D. Kendrick, "Freedom Scientific Focusing On Braille Part 2: A Review of the Focus Blue 40 Braille Display,"  
480 *American Foundation for the Blind Magazine*, vol. 15, no. 9, pp. 2-3, 2014.
- 481 [3] HyperBraille; [Online]. Available: <http://web.metec-ag.de/graphikdisplay.html>.
- 482 [4] National Federation of the Blind, "The braille literacy crisis in America: Facing the truth, reversing the trend,  
483 empowering the blind"; [Online]. Available: <http://www.nfb.org>.

- 484 [5] L. Yobas, D. M. Durand, G. G. Skebe, F. J. Lisy, and M. Huff, "A novel integrable microvalve for refreshable  
485 Braille display system," *Journal of Microelectromechanical Systems*, vol. 12, no. 3, pp. 252-263, 2003.
- 486 [6] Y. Haga, W. Makishi, K. Iwami, K. Totsu, K. Nakamura, and M. Esashi, "Dynamic Braille display using SMA  
487 coil actuator and magnetic latch," *Sensors and Actuators A: Physical*, vol. 119, no. 2, pp. 316-322, 2005.
- 488 [7] K. Ren, S. Liu, M. Lin, Y. Wang, and Q. Zhang, "A compact electroactive polymer actuator suitable for  
489 refreshable Braille display," *Sensors and Actuators A: Physical*, vol. 143, no. 2, pp. 335-342, 2008.
- 490 [8] P. Chakraborti, H. K. Toprakci, P. Yang, N. Di Spigna, P. Franzon, and T. Ghosh, "A compact dielectric  
491 elastomer tubular actuator for refreshable Braille displays," *Sensors and Actuators A: Physical*, vol. 179, pp.  
492 151-157, 2012.
- 493 [9] P. Brochu, and Q. Pei, "Advances in dielectric elastomers for actuators and artificial muscles," *Macromolecular*  
494 *Rapid Communications*, vol. 31, no. 1, pp. 10-36, 2010.
- 495 [10] F. Carpi, D. De Rossi, R. Kornbluh, R. E. Pelrine, and P. Sommer-Larsen, *Dielectric Elastomers as*  
496 *Electromechanical Transducers: Fundamentals, Materials, Devices, Models and Applications of an Emerging*  
497 *Electroactive Polymer Technology*, Oxford: Elsevier, 2008.
- 498 [11] R. Pelrine, R. Kornbluh, Q. Pei, and J. Joseph, "High-speed electrically actuated elastomers with strain greater  
499 than 100%," *Science*, vol. 287, no. 5454, pp. 836-839, 2000.
- 500 [12] F. Carpi, *Electromechanically Active Polymers: A Concise Reference*, Zurich: Springer International Publishing,  
501 2016.
- 502 [13] F. Carpi, and E. Smela, *Biomedical Applications of Electroactive Polymer Actuators*, Chichester: John Wiley &  
503 Sons, 2009.
- 504 [14] F. Carpi, S. Bauer, and D. De Rossi, "Stretching dielectric elastomer performance," *Science*, vol. 330, no. 6012,  
505 pp. 1759-1761, 2010.
- 506 [15] N. Di Spigna, P. Chakraborti, D. Winick, P. Yang, T. Ghosh, and P. Franzon, "The integration of novel EAP-  
507 based Braille cells for use in a refreshable tactile display," in *Proc. of SPIE*, Vol., 7642, 2010, pp. 76420A-  
508 76420A-9.
- 509 [16] R. Heydt, and S. Chhokar, "Refreshable Braille display based on electroactive polymers," in *Proc. 23rd Intl.*  
510 *Display Res. Conf.*, Phoenix, Arizona, 15-18 September, 2003, pp. 5.
- 511 [17] H. R. Choi, I. M. Koo, K. Jung, S.-g. Roh, J. C. Koo, J. Nam, and Y. K. Lee, "A Braille display system for the  
512 visually disabled using a polymer based soft actuator," In *Biomedical Applications of Electroactive Polymer*  
513 *Actuators*, F. Carpi, and E. Smela, Editors, pp. 427-442, Chichester: Wiley, 2009.

- 514 [18] H. S. Lee, H. Phung, D.-H. Lee, U. K. Kim, C. T. Nguyen, H. Moon, J. C. Koo, and H. R. Choi, "Design  
515 analysis and fabrication of arrayed tactile display based on dielectric elastomer actuator," *Sensors and Actuators*  
516 *A: Physical*, vol. 205, pp. 191-198, 2014.
- 517 [19] M. Matysek, P. Lotz, and H. F. Schlaak, "Tactile display with dielectric multilayer elastomer actuators," in *Proc.*  
518 *of SPIE*, Vol. 7287, 2009, pp. 72871D-72871D-9.
- 519 [20] Z. Yu, W. Yuan, P. Brochu, B. Chen, Z. Liu, and Q. Pei, "Large-strain, rigid-to-rigid deformation of bistable  
520 electroactive polymers," *Applied Physics Letters*, vol. 95, no. 19, pp. 192904, 2009.
- 521 [21] F. Carpi, G. Frediani, and D. De-Rossi, "Hydrostatically coupled dielectric elastomer actuators," *IEEE/ASME*  
522 *Transactions on Mechatronics*, vol. 15, no. 2, pp. 308-315, 2010.
- 523 [22] S. J. A. Koh, T. Li, J. Zhou, X. Zhao, W. Hong, J. Zhu, and Z. Suo, "Mechanisms of large actuation strain in  
524 dielectric elastomers," *Journal of Polymer Science Part B: Polymer Physics*, vol. 49, no. 7, pp. 504-515, 2011.
- 525 [23] L. Mullins, "Softening of rubber by deformation," *Rubber Chemistry and Technology*, vol. 42, no. 1, pp. 339-  
526 362, 1969.
- 527 [24] F. Carpi, I. Anderson, S. Bauer, G. Frediani, G. Gallone, M. Gei, C. Graaf, C. Jean-Mistral, W. Kaal, G. Kofod,  
528 M. Kollosche, R. Kornbluh, B. Lassen, M. Matysek, S. Michel, S. Nowak, B. O'Brien, Q. Pei, R. Pelrine, B.  
529 Rechenbach, S. Rosset, and H. Shea, "Standards for dielectric elastomer transducers," *Smart Materials and*  
530 *Structures*, vol. 24, no. 10, pp. 105025-1 – 105025-25, 2015.
- 531 [25] P. Mousty, and P. Bertelson, "A study of braille reading: 1. Reading speed as a function of hand usage and  
532 context," *The Quarterly Journal of Experimental Psychology*, vol. 37, no. 2, pp. 217-233, 1985.
- 533 [26] Web search: "Average word length in the English language"; [Online]. Available:  
534 <http://www.wolframalpha.com/input/?i=average+word+length+English+language>.
- 535 [27] G. Frediani, D. Mazzei, D. De Rossi, and F. Carpi, "Wearable wireless tactile display for virtual interactions  
536 with soft bodies," *Frontiers in Bioengineering and Biotechnology*, vol. 2, Article 31, pp. 1-7, 2014.
- 537 [28] I. Koo, K. Jung, J. Koo, J. D. Nam, Y. Lee, and H. R. Choi, "Wearable fingertip tactile display," in *Proc. of 2006*  
538 *Sice-Icase International Joint Conference*, Busan, 2006, pp. 1911-1916.
- 539 [29] F. B. Madsen, A. E. Daugaard, S. Hvilsted, and A. L. Skov, "The Current State of Silicone-Based Dielectric  
540 Elastomer Transducers," *Macromolecular Rapid Communications*, vol. 37, no. 5, pp. 378-413, 2016.
- 541 [30] S. J. Dünki, Y. S. Ko, F. A. Nüesch, and D. M. Opris, "Self-Repairable, High Permittivity Dielectric Elastomers  
542 with Large Actuation Strains at Low Electric Fields," *Advanced Functional Materials*, vol. 25, no. 16, pp. 2467-  
543 2475, 2015.

- 544 [31] L. Maffli, S. Rosset, M. Ghilardi, F. Carpi, and H. Shea, "Ultrafast All-Polymer Electrically Tunable Silicone  
545 Lenses," *Advanced Functional Materials*, vol. 25, no. 11, pp. 1656-1665, 2015.
- 546 [32] A. Poulin, S. Rosset, and H. R. Shea, "Printing low-voltage dielectric elastomer actuators," *Applied Physics*  
547 *Letters*, vol. 107, no. 24, pp. 244104, 2015.